MENTATION PAGE

Form Approved
OMB No. 0704-0188

estimated to average 1 hour per response, including the time for reviewing instructions, searching existing data sources, g and reviewing the collection of information. Send comments regarding this burden estimate or any other aspect of this g this burden, to Washington Headquarters Services, Directorate for information Operations and Reports, 1215 Jefferson o the Office of Management and Budget, Paperwork Reduction Project (0704-0188), Washington, DC 20503

REPORT DATE	3. REPORT TYPE AND DATES COVERED
June 1994	Final 15 Jul 85-28 Feb 91

4. TITLE AND SUBTITLE
Deformation, Strength, and Failure Modes of Laminated Conventional and Hybrid Polymer-Matrix Composites Loaded in the Thickness Direction

5. FUNDING NUMBERS
DAAG29-85-K-0195

6. AUTHOR(S)
A.A. Fahmy

7. PERFORMING ORGANIZATION NAME(S) AND ADDRESS(ES)
North Carolina State University
Raleigh, NC 27695

8. PERFORMING ORGANIZATION REPORT NUMBER

9. SPONSORING/MONITORING AGENCY NAME(S) AND ADDRESS(ES)
U.S. Army Research Office
P.O. Box 12211
Research Triangle Park, NC 27709-2211

10. SPONSORING/MONITORING AGENCY REPORT NUMBER
ARO 22339.3-MS

11. SUPPLEMENTARY NOTES
The views, opinions and/or findings contained in this report are those of the author(s) and should not be construed as an official Department of the Army position, policy, or decision, unless so designated by other documentation.

12a. DISTRIBUTION/AVAILABILITY STATEMENT
Approved for public release; distribution unlimited.

12b. DISTRIBUTION CODE

ABSTRACT *(Maximum 200 words)*

Thickness properties of laminated composites have not been as thoroughly investigated as in plane properties. Previous work by this investigator indicated that these properties, both elastic and strength, differ significantly from the transverse properties of unidirectional composites of the same materials system although the thickness direction is transverse to each play in the laminate.

(continued on reverse side)

14. SUBJECT TERMS	15. NUMBER OF PAGES
Composites, Laminated Composites, Laminates, Graphite-Epoxy, Kelvar-Epoxy, Glass-Epoxy, Hybrid Composites	47
	16. PRICE CODE

17. SECURITY CLASSIFICATION OF REPORT	18. SECURITY CLASSIFICATION OF THIS PAGE	19. SECURITY CLASSIFICATION OF ABSTRACT	20. LIMITATION OF ABSTRACT
UNCLASSIFIED	UNCLASSIFIED	UNCLASSIFIED	UL

NSN 7540-01-280-5500

Standard Form 298 (Rev. 2-89)
Prescribed by ANSI Std Z39-18
298-102

In this investigation the thickness properties of both — single system, and hybrid laminates are studied; namely, graphite-epoxy, kevlar-epoxy, glass-epoxy, graphite-epoxy/kevlar-epoxy, graphite-epoxy/glass-epoxy. However, knowledge of the in-plane properties of the laminates was also obtained since this was essential for the analysis and are also reported. Failure modes of the hybrid composites are characterized and discussed.

DISCLAIMER NOTICE

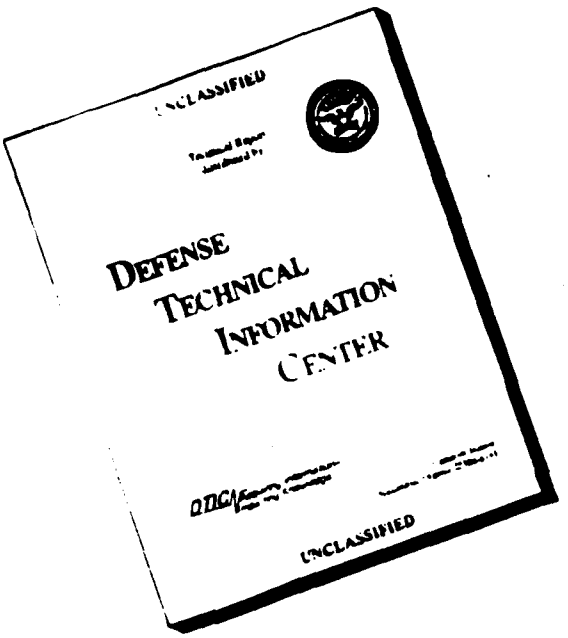

THIS REPORT IS INCOMPLETE BUT IS THE BEST AVAILABLE COPY FURNISHED TO THE CENTER. THERE ARE MULTIPLE MISSING PAGES. ALL ATTEMPTS TO DATE TO OBTAIN THE MISSING PAGES HAVE BEEN UNSUCCESSFUL.

223393-MS

Final Report on

DEFORMATION, STRENGTH, AND FAILURE MODES OF LAMINATED CONVENTIONAL AND HYBRID POLYMER-MATRIX COMPOSITES LOADED IN THE THICKNESS DIRECTION

Research conducted under Grant #DAAG 29-85-K-0195

by

A. A. Fahmy, Professor
Principal Investigator
Materials Science & Engineering Department
North Carolina State University
Raleigh, North Carolina

TABLE OF CONTENTS

ABSTRACT

Thickness properties of laminated composites have not been as thoroughly investigated as in plane properties. Previous work by this investigator indicated that these properties, both elastic and strength, differ significantly from the transverse properties of unidirectional composites of the same materials system although the thickness direction is transverse to each play in the laminate.

In this investigation the thickness properties of both — single system, and hybrid laminates are studied; namely, graphite-epoxy, kevlar-epoxy, glass-epoxy, graphite-epoxy/kevlar-epoxy, graphite-epoxy/glass-epoxy. However, knowledge of the in-plane properties of the laminates was also obtained since this was essential for the analysis and are also reported. Failure modes of the hybrid composites are characterized and discussed.

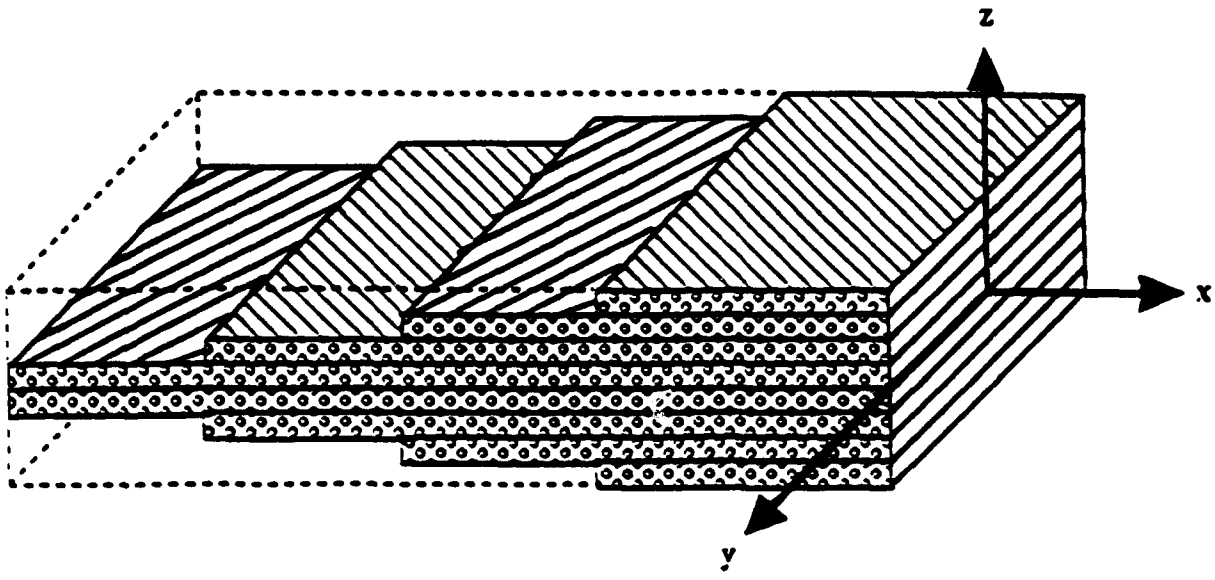

Fig. 1 Lay-up of an angle-ply laminate using unidirectional pre-preg tapes.

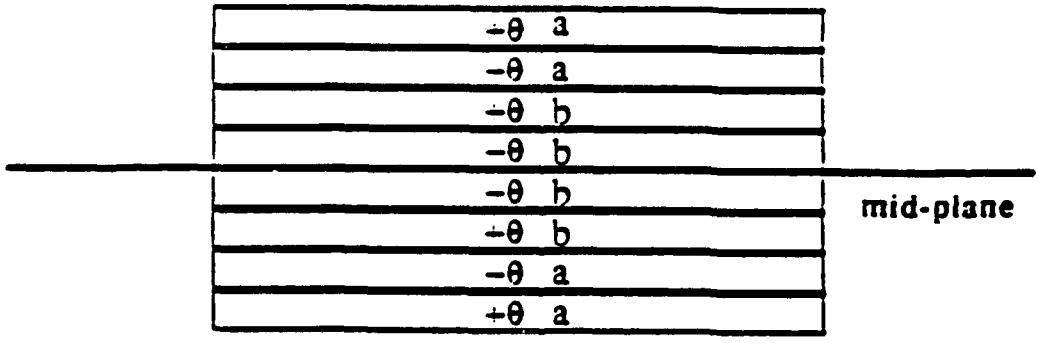

θ = off-axis angle

a, b = lamina system

Fig. 2 Stacking sequence for a balanced hybrid angle-ply laminate symmetric about its mid-plane.

I. EXPERIMENTAL

The experimental phase of this work consists primarily of determining:

1. The elastic constants involving the thickness direction of hybrid laminates.
2. Strength along their thickness direction.
3. Thermal expansion coefficients along the thickness direction of the laminates.

The elastic constants were determined both in tension and compression while the strength was determined in compression only. Specimens for compression loading were nearly cubical in shape with edges measuring approximately 1 1/2". In tension experiments a specially designed test specimen was used, referred to as the double ligament specimen, in which two ligaments were subjected to purely tensile stresses. The load in both cases was applied in an instron machine and the specimen were instrumented with electrical strain gages.

Also, in order that the experimental results may be compared with results of numerical analysis, unidirectional samples of the three fiber-resin systems were tested for their elastic and strength properties. Table 1 lists the elastic properties of these composites. Namely their longitudinal Youngs modulus E_L, transverse Youngs modulus E_T, shear modulus G_{LT}, the in-plane major Poisson's ratio ν_{LT}, the transverse-transverse Poisson's ration ν_{TT}. Table 2 lists the strength properties of the unidirectional composites, i.e. the longitudinal and transverse tensile strength X_T and Y_T, the longitudinal and transverse compressive strength X_C and Y_C as well as the in-plane shear strength T.

Values reported in Table 1 and 2 were obtained experimentally in our laboratory and may differ — slightly — from those reported by suppliers.

TABLE 1. Material Properties of Graphite-, Glass-, and Kevlar-Epoxy Matrix Composites*

	Graphite/Epoxy	Glass/Epoxy	Kevlar/Epoxy
E_L	17.83E6	6.24E6	10.46E6
E_T	1.02E6	1.77E6	.58E6
G_{LT}	.488E6	.471E6	.265E6
ν_{LT}	.36	.333	.428
ν_{TT}	.46	.43	.56

*T300 Graphite/Rigidite 5209 Resin

E-Glass/Rigidite 5216 Resin

Kevlar–49/Rigidite 5216 Resin

Values were determined by experiments in the lab

TABLE 2. Longitudinal and Transverse Strengths in Tension, Compression, and Shear Strengths of Graphite-, Glass-, and Kevlar-Epoxy Matrix Composites

	Graphite/Epoxy	Glass/Epoxy	Kevlar/Epoxy
X_T*	215,000**	186,400	210,100
X_C	–107,900	–75,500	–34,600
Y_T	8,400	7,200	3,210
Y_C	–38,270	–31,270	–17,900
S	16,270	15,360	9,633

*X : Longitudinal Direction

Y : Transverse Direction

T : Tension

C : Compression

S : Shear Strength

** : Unit (psi)

1. Elastic Properties

A. In Compression:

Two sets of samples of each of the ply-angles were tested. One set was for the determination of E_3, ν_{31} and ν_{32} by applying a compressive load in the thickness direction. The other was for obtaining stress-strain diagrams to failure under compression in the same direction. The samples for the elastic moduli determination were cubes, approximately 1 1/2" on edge and were instrumented with strain gauges, namely 0/90° double gauge rosettes type EA 06–125TM–120 series. An Instron machine was used with a crosshead speed of .02 inch per minute. Two digital strain indicators, a Vishay VE20 A and a BLH model 1200, were used to measure the strain. The compressive load was applied and increased until a strain ε_3 reached approximately 1000×10^{-6} and ε_2 and ε_3 were recorded throughout.

Experimental values of E_3, ν_{31} and ν_{32} for the graphite-epoxy/kevlar-epoxy samples and for the graphite-epoxy/glass-epoxy samples are given in Table 3 and 4 respectively as well as Fig. 3 and 4.

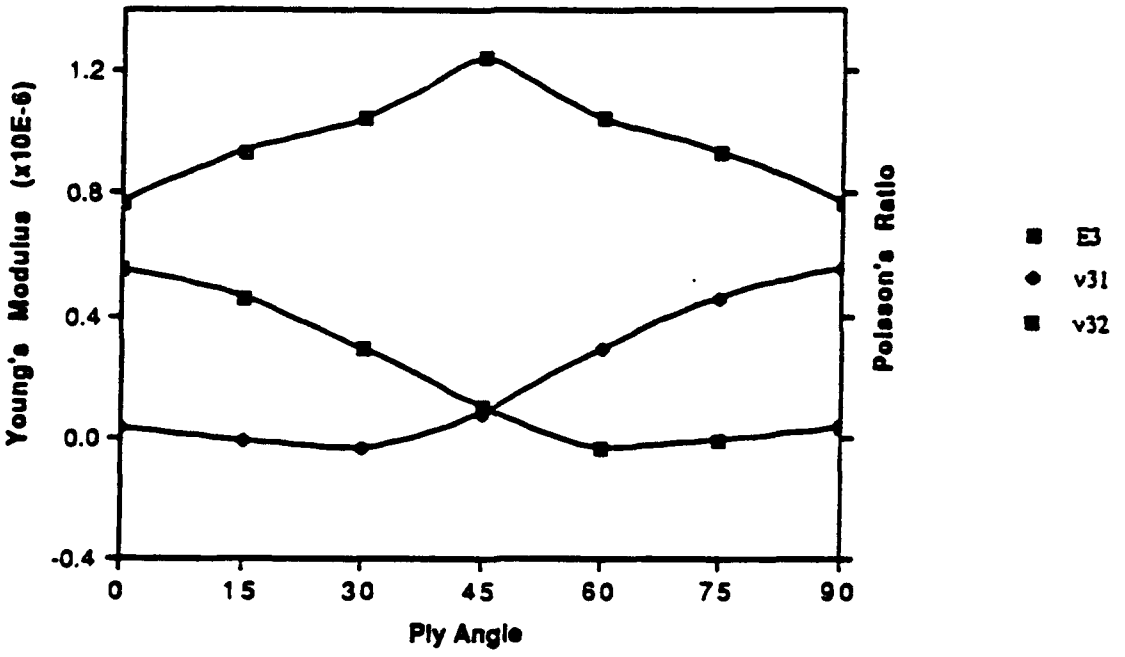

Fig. 3 E_3, n_{31}, and n_{32} of the Graphite-epoxy/Kevlar-epoxy Laminate vs Ply-angle.

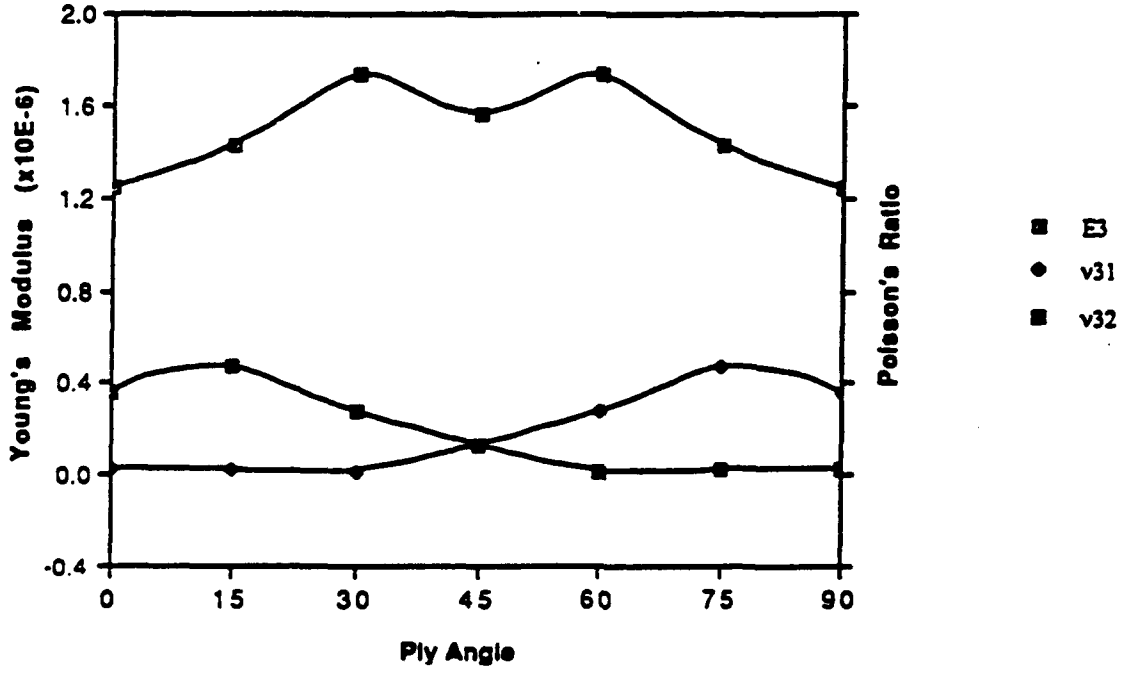

Fig. 4 E_3, v_{31}, and v_{32} of the Graphite-Epoxy / Glass-Epoxy Laminate vs Ply-angle.

B. In Tension

The samples used here were the double ligament tensile sample illustrated in Fig. 5. The sample blank was a block .4" x .4" x 2" and two ligaments were formed by cutting in slots from the top and bottom of the sample blank. A special jig held both sides of the sample firmly while the center portion was pushed by a square punch .4" x .4". The two ligaments were thus subjected each to a tensile load equal to one-half of the applied load and the strain was recorded using electrical strain gages as illustrated in Fig. 6.

Youngs' modulus in the thickness direction for the 3 hybrid systems as a function of ply angle is shown in Fig. 7, 8, and 9.

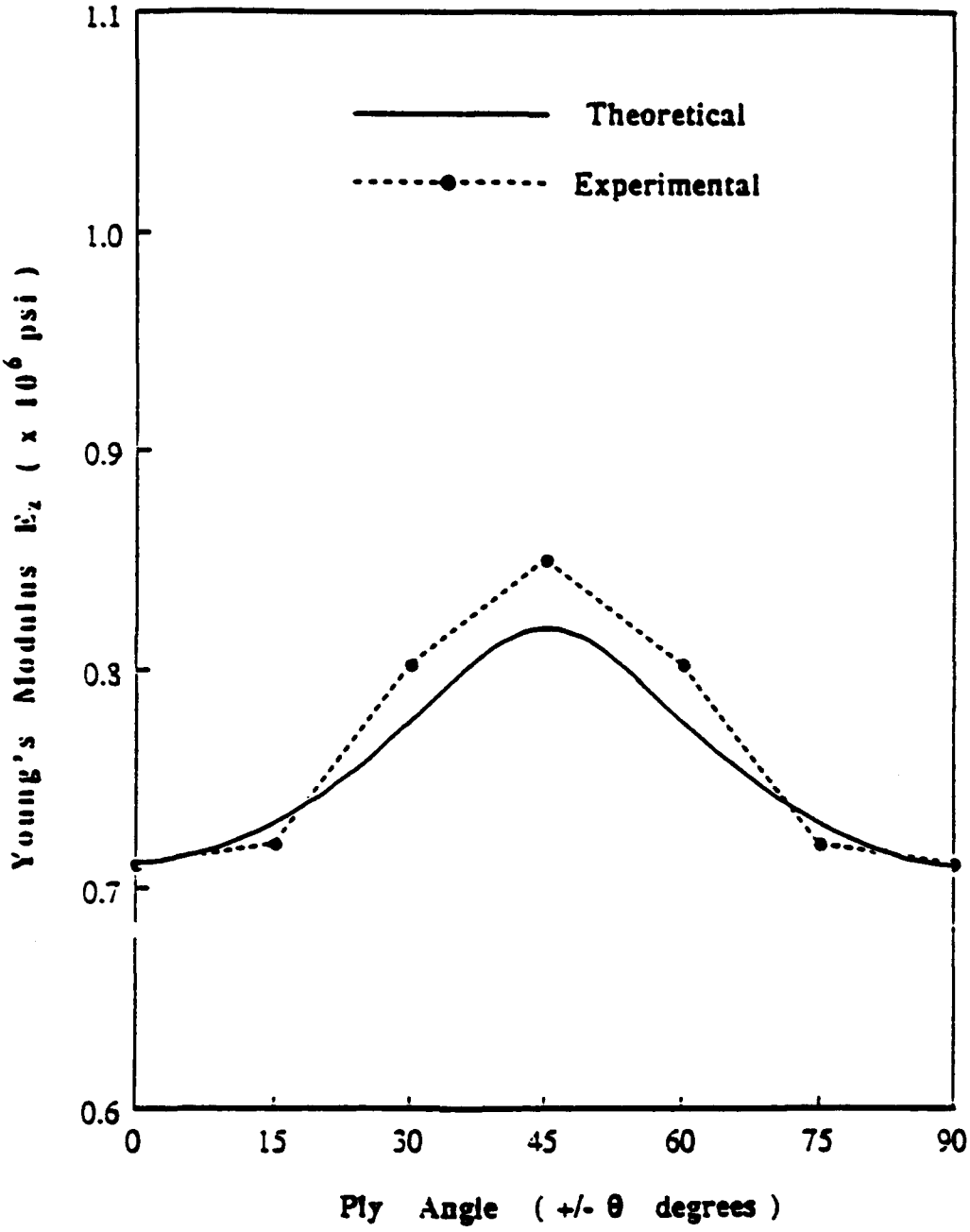

Fig. 7 Comparison between experimental and theoretical through-the-thickness Young's moduli for angle-ply T300 Graphite, Kevlar 49C / Epoxy hybrid laminates.

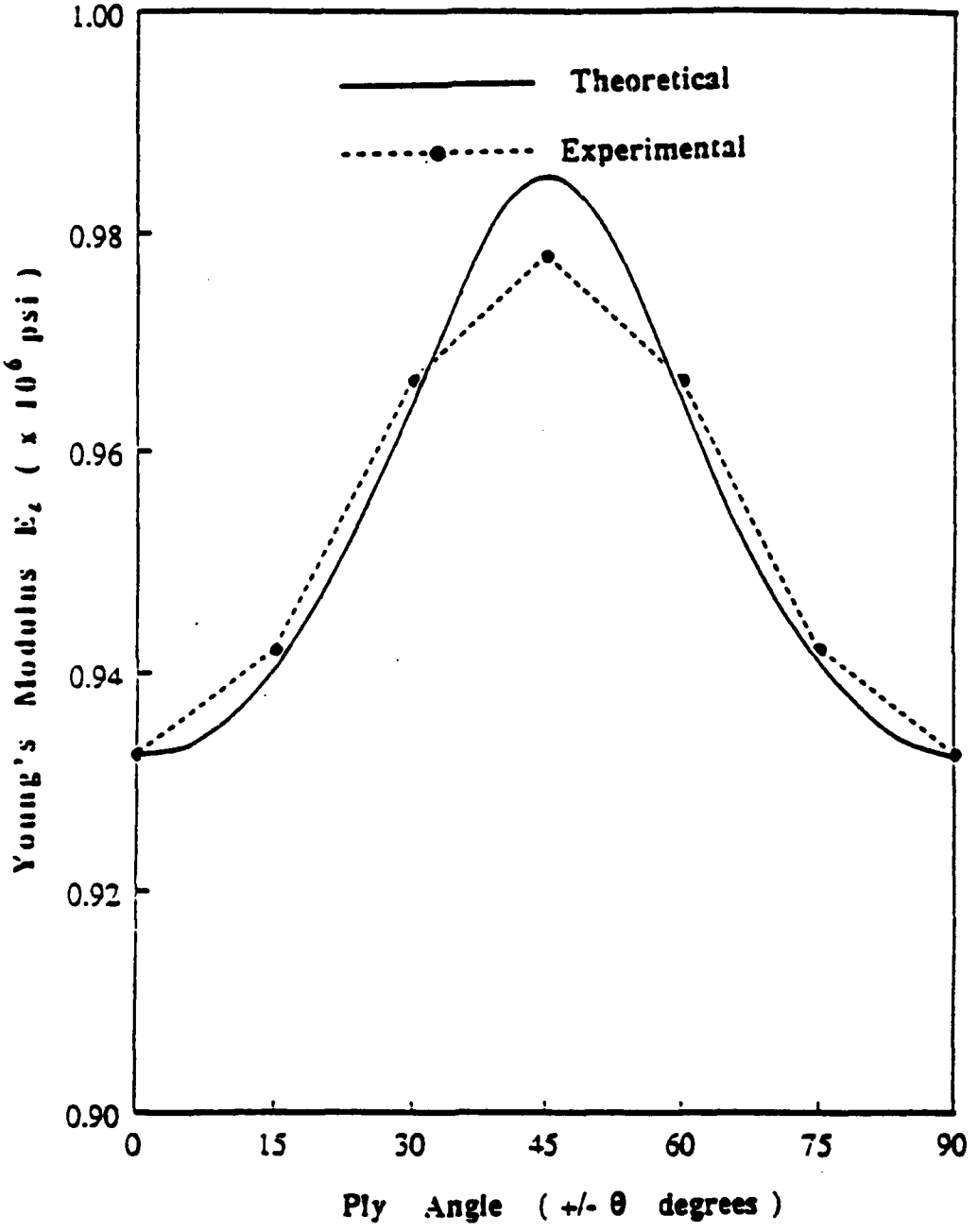

Fig. 8 Comparison between experimental and theoretical through-the-thickness Young's moduli for angle-ply Kevlar 49C, E-Glass / Epoxy hybrid laminates.

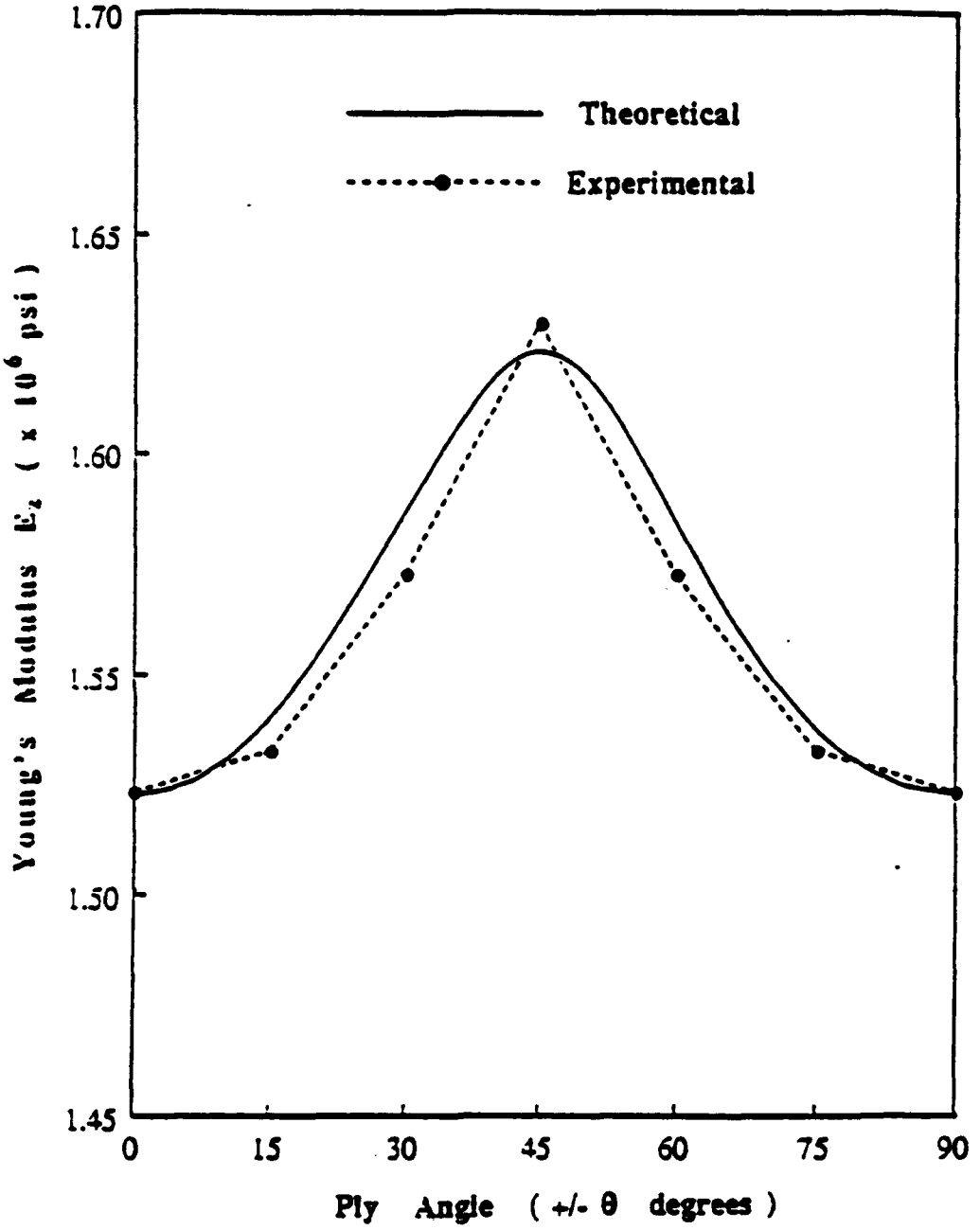

Fig. 9 Comparison between experimental and theoretical through-the-thickness Young's moduli for angle-ply E-Glass, T300 Graphite / Epoxy hybrid laminates.

2. Strength (Stress-Strain Behavior)

Compression tests were performed on a series of angle-ply hybrid laminates loaded along the thickness direction for each of the two hybrid systems graphite-epoxy/kevlar-epoxy and graphite-epoxy/glass-epoxy. A Tinius-Olsen 60,000 lb capacity hydraulic machine was used for these tests and the sample contraction was monitored with a .001 inch dial gauge.

The stress-strain diagrams for each series were platted on the same axes and shown in Fig. 10 and Fig. 11. It can be seen that the ply angle greatly influences the stress-strain behavior. Inspection of these diagrams indicates that — for both systems — the fracture strength increased as the ply angle changed from 0° to 45° and that the ± 45° laminates stayed essentially linear elastic to failure, while there was considerable plastic contraction in other samples particularly the ± 15° laminates.

Tensile tests on a conventional tensile samples were not performed and those performed on the double ligament samples showed premature failures due to the stress concentration at the slot ends and the brittle nature of the material.

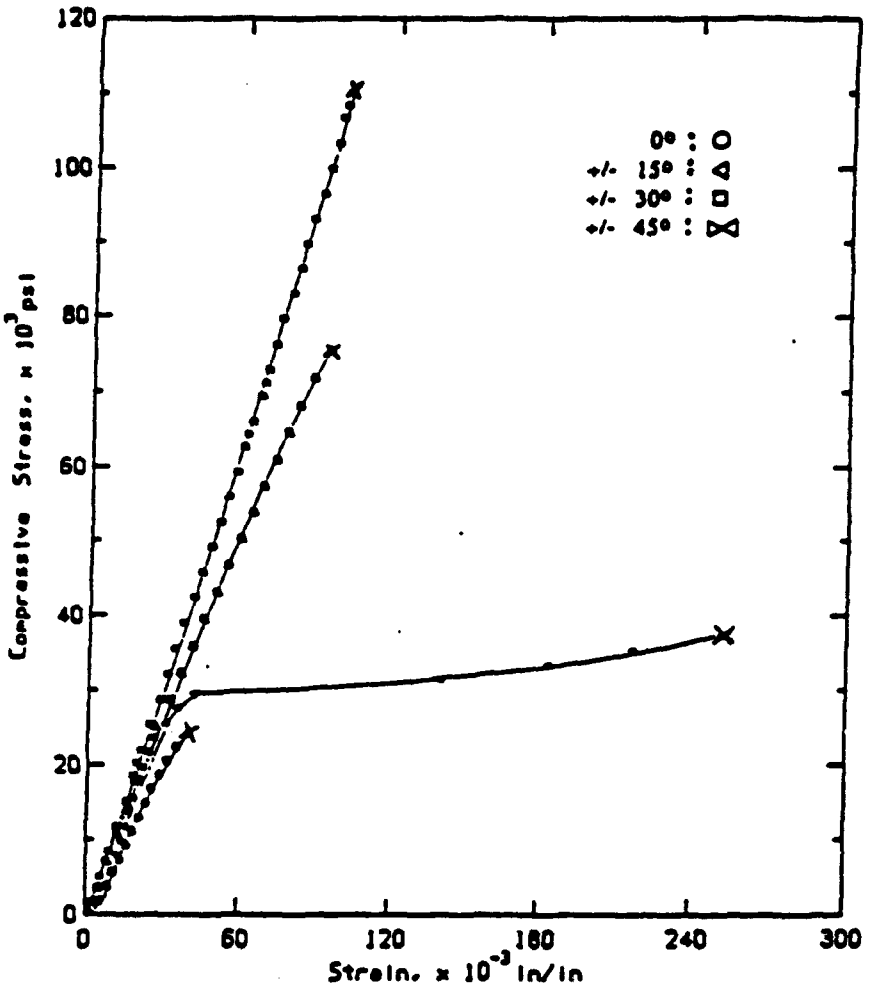

Fig. 10 Stress-Strain diagram of Graphite-Epoxy / Kevlar-Epoxy hybrid laminates compressed along the thickness direction.

3. Failure Modes

The failed specimens showed very different failure modes depending on their ply-angle. The three primary modes of failure observed in the fracture of angle-ply laminates are fiber separation, fiber breakage, and ply delamination. Total failure of a laminate can occur by any combination of these three modes.

The lateral compressive strength is dominated by matrix properties and failure generally occurs by shear on planes containing the fiber direction. The fibers act as stress raisers and their effect is detrimental only with nonductile matrices. For ductile matrices, the strength of the composite is not much different from the strength of the matrix. The crack travels primarily in the matrix and occasionally along the fiber-matrix interface. However, in rare instances, the crack has been known to go through a fiber, breaking it longitudinally, i.e. parallel to the fiber axis shown in Fig. 12.

In order for lateral compressive fracture to occur in each ply of a laminated composite, the crack has to change its plane as it goes from ply to ply. This occurrence may be feasible if the orientations of fibers in adjacent plies are not very different. If, however, the difference in orientation is large, it is conceivable that it may be easier for fibers to break crosswise and thus affect or control the compressive strength. The failed angle-ply laminates showed that the adjacent layers in +/- θ° tended to rotate in the direction that bisects the obtuse angle between fibers under the compression along the thickness direction, showing a "reverse scissoring effect" and, consequently, changing their ply-angle toward +/- 45° while isotropic materials barrel in lateral directions perpendicular to the compression axis. This may explain the four fold increase of failure strength of the angle-ply laminate as the ply angle increased from 0° to +/- 45°. These effects are shown in the fractographs of the specimens.

The 0° graphite-epoxy/kevlar-epoxy hybrid laminate in Fig. 13 shows that the fracture occurred in the matrix and that the fracture surface is parallel or nearly parallel to the fiber direction and shows smooth fracture path without fiber pull out or delamination. Another view of the same specimen in Fig. 14 shows that the crack traveled in a more or less straight path in the graphite layers, but shows a zigzag pattern in the kevlar layers. Fig. 15 is of the failed +/- 15° graphite-epoxy/kevlar-epoxy hybrid laminate with a shear plane at 45° with the compression axis. It also shows a noticeable contraction on the sides in the 0° direction while the other sides are barrelled. Examination of the fractured specimen showed that on the upper and lower surfaces the ply angle reached +/- 31° (i.e. 62° between fibers) while in the middle of the mid layers on the fractured surfacae, ply angle of fibers in adjacent plies were almost 90°. This specimen showed a negative Poisson's ratio by an experiment and by computer analysis performed with ELAS. Fig. 16 is of a side surface of the same specimen showing a tendency of the kevlar fibers to be pulled out, and of the graphite fibers to be broken at the surface. A close-up view of the fractured surface (see Fig. 17) shows shifted fiber direction. The kevlar fibers are pulled out, and their ply angle changed from +/- 15° to +/- 31°. Fig. 18 shows transverse cracking in the graphite layers while none is seen on the kevlar layers. This took place because the graphite fibers are brittle while the kevlar fibers are ductile and expand more than graphite fibers. The cracks started at the interface between the graphite and kevlar layers and developed inwardly to the interface of graphite layers. But since the graphite layers are actually double layers of +/- 15°, the top and bottom layers tend to rotate in opposite directions, causing the transverse crack to be S shaped as shown in the figure. In Fig. 19, the +/- 30° graphite-epoxy/kevlar-epoxy hybrid laminate shows delamination between the graphite and kevlar layers and resins

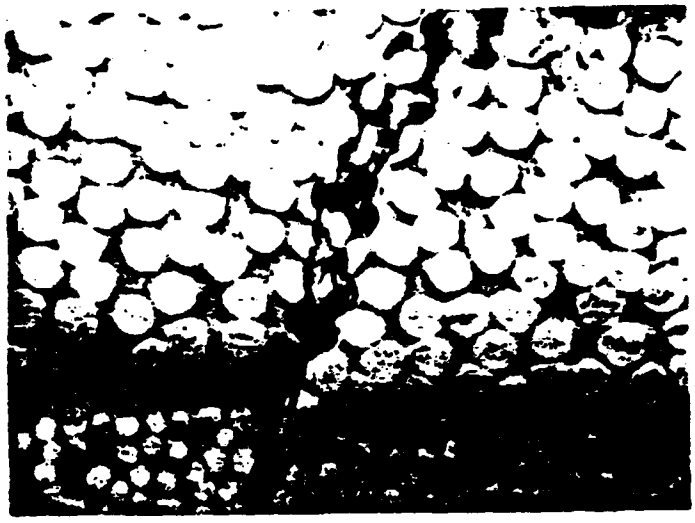

Fig. 12 Longitudinal cracks on the 0 Kevlar fibers (Mag. x440).

Fig. 13 Side surface of the fractured 0 Graphite-Epoxy / Kevlar-Epoxy hybrid laminate (Mag. x30).

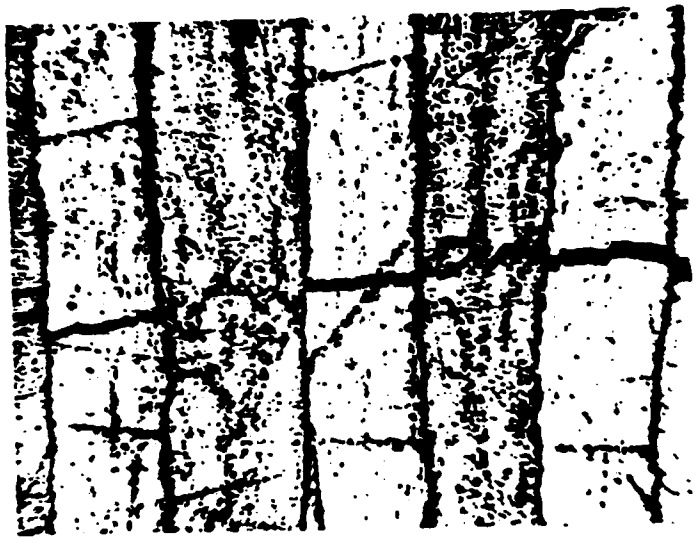

Fig. 14 Crack on the fractured 0 Graphite-Epoxy / Kevlar-Epoxy hybrid laminate (Mag. x50).

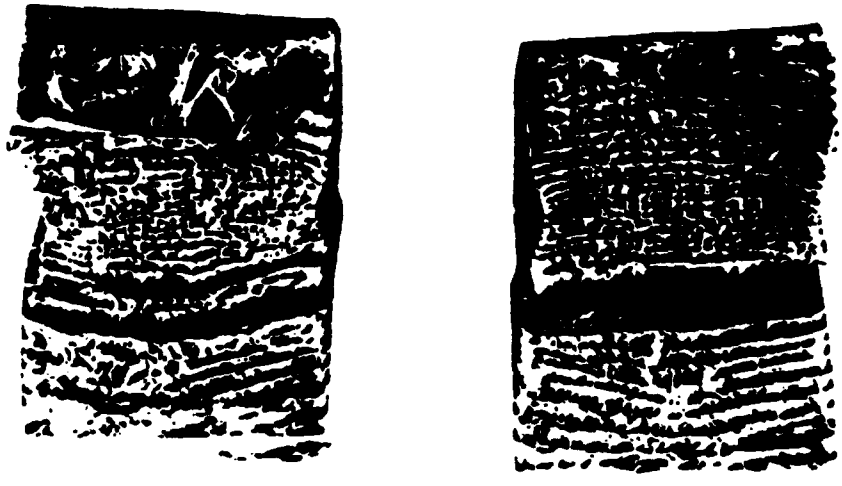

Fig. 15 Fractured specimen of the +/- 15 Graphite-Epoxy / Kevlar-Epoxy hybrid laminate (Mag. x2).

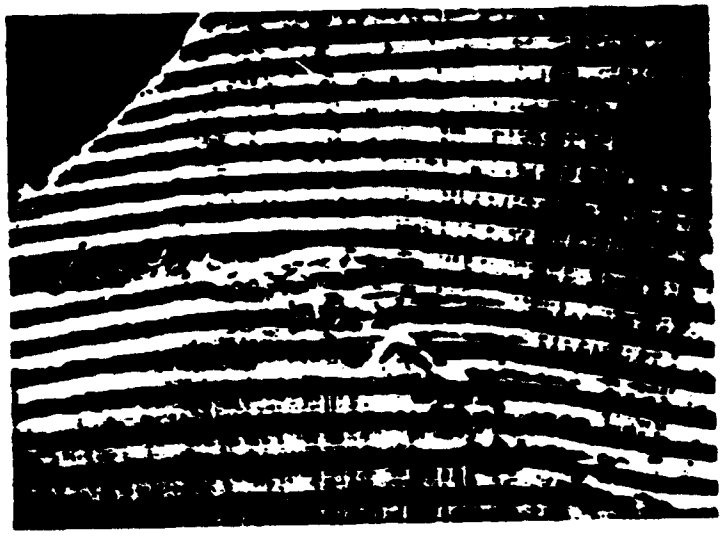

Fig. 16 Delamination of Kevlar layers in the +/- 15 Graphite-Epoxy / Kevlar-Epoxy hybrid laminate (Mag. x12).

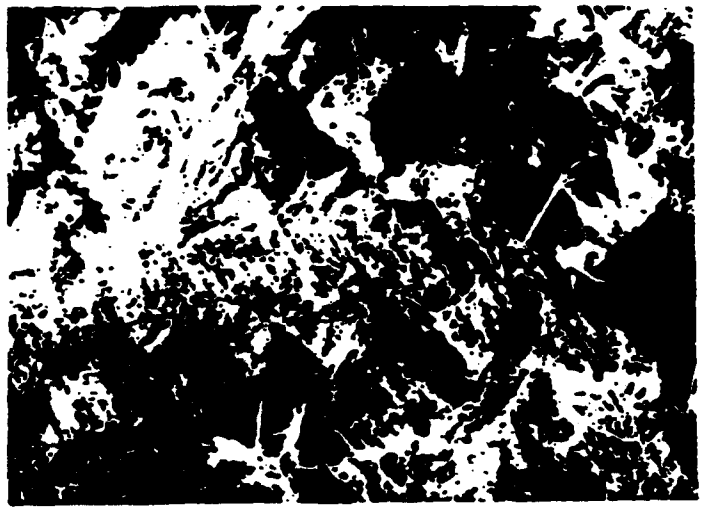

Fig. 17 Angle change of fibers in the +/- 15 Graphite-Epoxy / Kevlar-Epoxy hybrid laminate (Mag. x30).

Fig. 18 Transverse cracking in the graphite layers of the +/- 15 Graphite-Epoxy / Kevlar-Epoxy hybrid laminate (mag. x50).

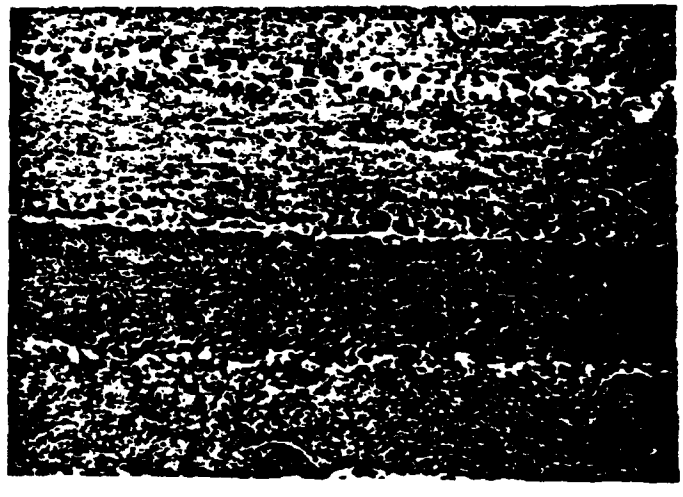

Fig. 19 Delamination and resin squeeze out in the +/- 15 Graphite-Epoxy / Kevlar-Epoxy hybrid laminate (Mag. x100).

which are not ductile in regular conditions were squeezed out between layers. The failed +/- 45° graphite-epoxy/kevlar-epoxy hybrid laminate (see Fig. 20) shows delamination and pull-out of kevlar fibers. The kevlar fibers also show fibrillation. This laminate did not show any angle change until failure. When this specimen failed under compression in the thickness direction, broken pieces were ejected sideways explosively. The same failure mode was observed on the graphite-epoxy/glass-epoxy hybrid laminate of the same angle and the failed surface which shows no change of fiber orientation is shown clearly in Fig. 27. Fig. 21 shows that the fibers in the +/- 45° graphite-epoxy/kevlar-epoxy hybrid laminate failed in tension with no angle change in orientation. Fig. 22 illustrates the side surface of the same specimen which shows the kevlar fibers protruding particularly close to the interface between the two kevlar-epoxy plies and the resin squeezed out between layers.

These trends are similar for graphite-epoxy/glass-epoxy hybrid laminates, too. Fig. 23 illustrates the side view of the failed 0° graphite-epoxy/glass-epoxy hybrid laminate which shows matrix failure and cracks that make approximately a 30° angle to the compression direction. This specimen also shows a fairly clean crack path in the graphite fiber layers while multiple cracking and a jagged crack path are seen in the glass fiber layers in Fig. 24. Fig. 25 shows a shear crack at 45° to the compression direction in the +/- 15° graphite-epoxy/glass-epoxy hybrid laminate. The light area on both sides of the crack is due to the local edge effect. The contraction of side surfaces is not as evident here as in the graphite-epoxy/kevlar-epoxy hybrid laminate of the same angle. Fig. 26 shows the fractured surfaces of the +/- 15° graphite-epoxy/glass-epoxy hybrid laminate which have a plateau caused by delamination between the glass fiber layers near the midplane of the specimen. The direction of the glass fibers on each plateau is

opposite and shows that delamination occurred between the +15* and -15° glass fiber layers. Fig. 27 shows a fractured surface of the +/- 45° graphite-epoxy/glass-epoxy hybrid laminate by delamination and fiber breakage without any angle change.

To interpret the fracture mechanism, it has been explained that in the vicinity of the free edge of certain angle-ply finite-width tensile coupons, large, nonlinear shear strains occur at the interfaces of fiber orientations leading to near maximum shear coupling compliance while the strength of other fiber orientations are predicted by lamination strength theories. Their arguments state that at the point of interlaminar shear failure, the laminae are free from interlaminar shear strain. When the interlaminar shear stress at the interface is near the ultimate capacity of the material, the inherent nonlinearity of the interlaminar shear stress-strain behavior produces a state of strain within the laminae which is virtually free from interlaminar shear strain. Hence, the interlaminar shear strain is concentrated at the interfaces between lamina of + θ and - θ degree fiber orientations, and these strains allow the initiation of matrix cracks at the free edge which are ultimately responsible for the premature rupture of the coupon.

The highest intensity of such strain in the principal direction of the layers is for the +/- 15° laminate and the lowest intensity is for the +/- 45°. Hence, it would appear that rupture of the +/- 45° laminate is not sensitive to the state of stress and strain at the free edge, while rupture of the +/- 15° laminate is initiated at the free edge. This explains why lower angle-ply laminates changed their ply-angle while the +/- 45° laminate did not show any angle-change at all until failure. The mechanism postulated that the premature rupture is initiated by a large

Fig. 20 Delamination and fiber pull-out in the +/- 45 Graphite-Epoxy / Kevlar-Epoxy hybrid laminate and fibrillation of Kevlar fibers (Mag. x12).

Fig. 21 Tensile failure of fibers in the +/- 45 Graphite-Epoxy / Kevlar-Epoxy hybrid laminate (Mag. x40).

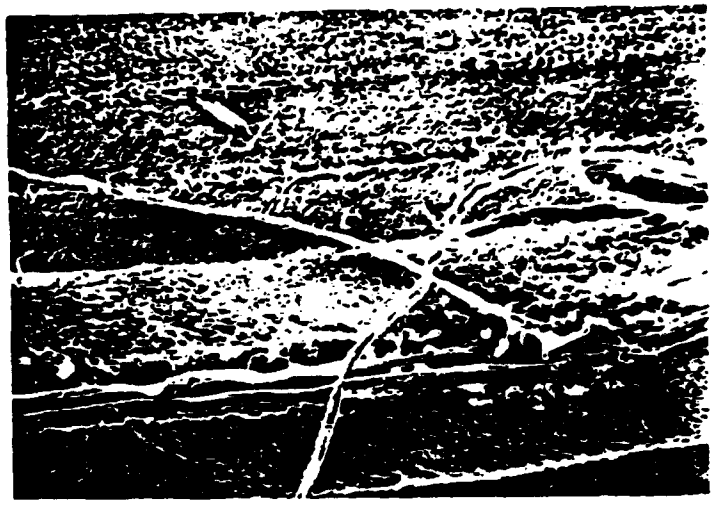

Fig. 22 Delamination and fiber separation of Kevlar layers in the +/- 45 Graphite-Epoxy / Kevlar-Epoxy hybrid laminate (Mag. x500).

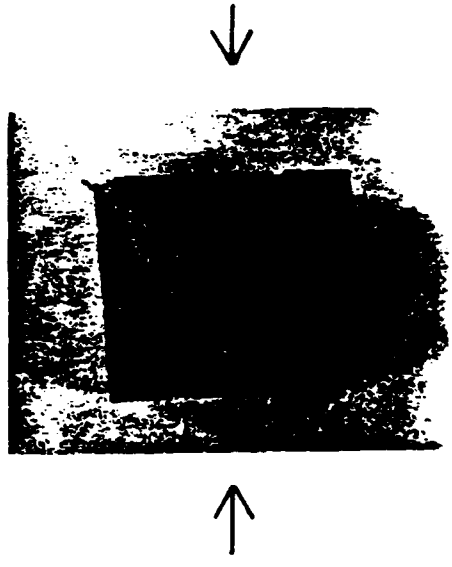

Fig. 23 Failure of the 0 Graphite-Epoxy / Glass-Epoxy hybrid laminate (Mag. x17)

Fig. 24 Close-up view of the surface of the failed 0 Graphite-Epoxy / Glass-Epoxy hybrid laminate (Mag. x40)

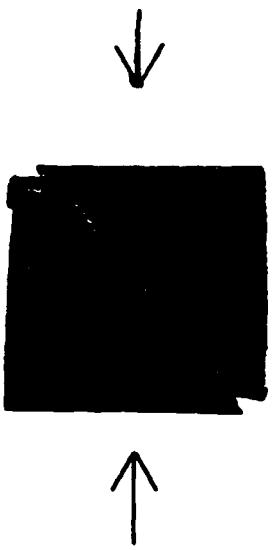

Fig. 25 Fracture in shear mode to the compression direction of the +/- 15 Graphite-Epoxy / Glass-Epoxy hybrid laminate (Mag. x1.7)

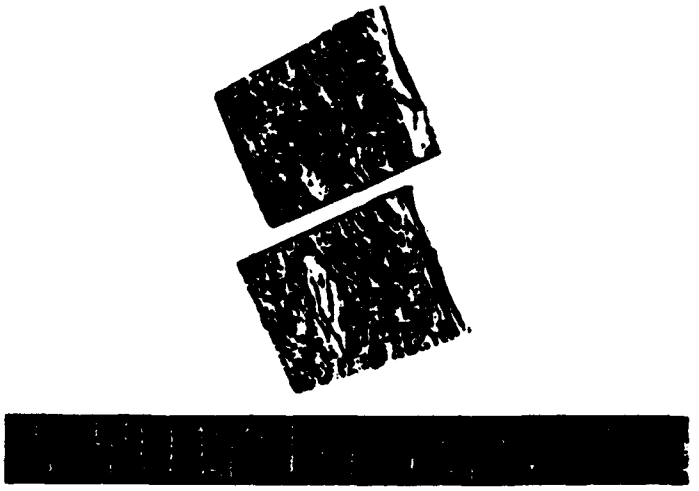

Fig. 26 Fractured surfaces of the +/- 15 Graphite-Epoxy / Glass-Epoxy hybrid laminate (Mag. x1.25)

Fig. 27 Fractured surfaces of the +/- 45 Graphite-Epoxy / Glass-Epoxy hybrid laminate (Mag. x1.7). Compression direction is perpendicular to the paper surface.

interlaminar shear stress at the interface which produces matrix cracks at the free edge. These cracks then propagate into the specimen and cause rupture.

II. ANALYTICAL

1. Stress Analysis of Hybrid Laminates in Compression

To verify the experimental results, a finite element analysis was performed. The model for this analysis is shown in Fig. 28. It has four plies of orientation $+\theta$ and $-\theta$ of two different composite systems. The general purpose computer program ELAS developed by Dr. S. Utku was used. Input data consisted of the number of nodes (20), the number of elements (four), the number of degrees of freedom at each node (three), the number and properties of materials (here, we had four materials, i.e. each layer of $+\theta$ and $-\theta$ orientation of each of the two composite systems was considered a different material since each had different stiffness values in the laminate coordinate system), and a uniform pressure was applied in the z-direction.

Every surface was restrained to remain flat and the inside nodes from node numbers 5 to 16 were free to move vertically. Node 17 was used a standard on the z-axis for nodes on the top surface, node 2 on the y-axis is for nodes on the plane of 2–4–20–18, and node 1 was fixed at the origin. Nodes 2 and 3 were free to move on the y- and x-axes, respectively. Dimensions for the model are 2 x 1 x 2 inches for graphite-epoxy/kevlar-epoxy hybrid laminates. These dimensions were detected to be consistent with the ply thickness obtained from the three prepreg tapes used in the experimental study.

From the resulting deflections, the values of E_3, ν_{12}, ν_{23}, and ν_{31} were calculated for each of the ply angles in each of the two hybrid laminates. Results of this analysis are given in Figs. 29 and 30 for Poisson's ratios, in Figs. 31 and 32 for E_1, E_2, and E_3, and for clarity, E_3 is given separately on Figs. 33 and 34.

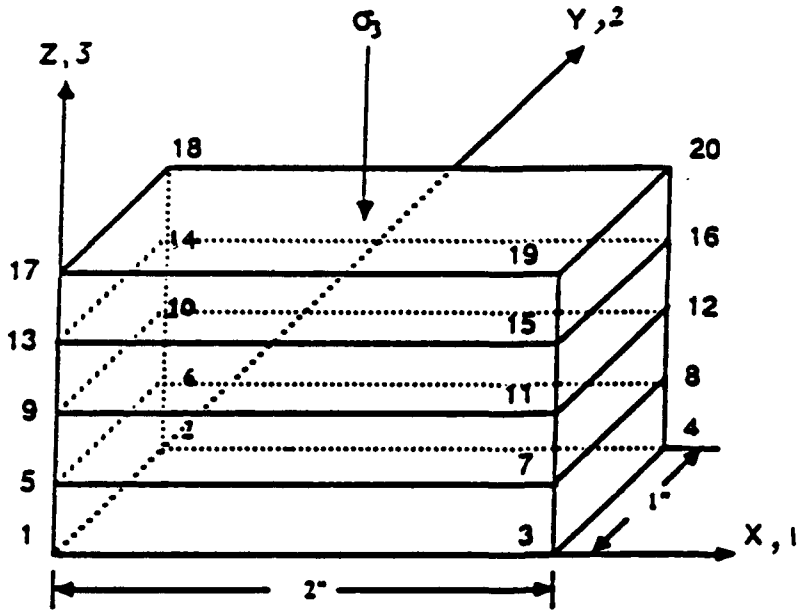

Fig. 28 Geometry of the model of a 4-ply hybrid laminate for a finite element method by ELAS.

	Height
Graphite-Epoxy / Glass-Epoxy:	2.5"
Graphite-Epoxy / Kevlar-Epoxy:	2.0"

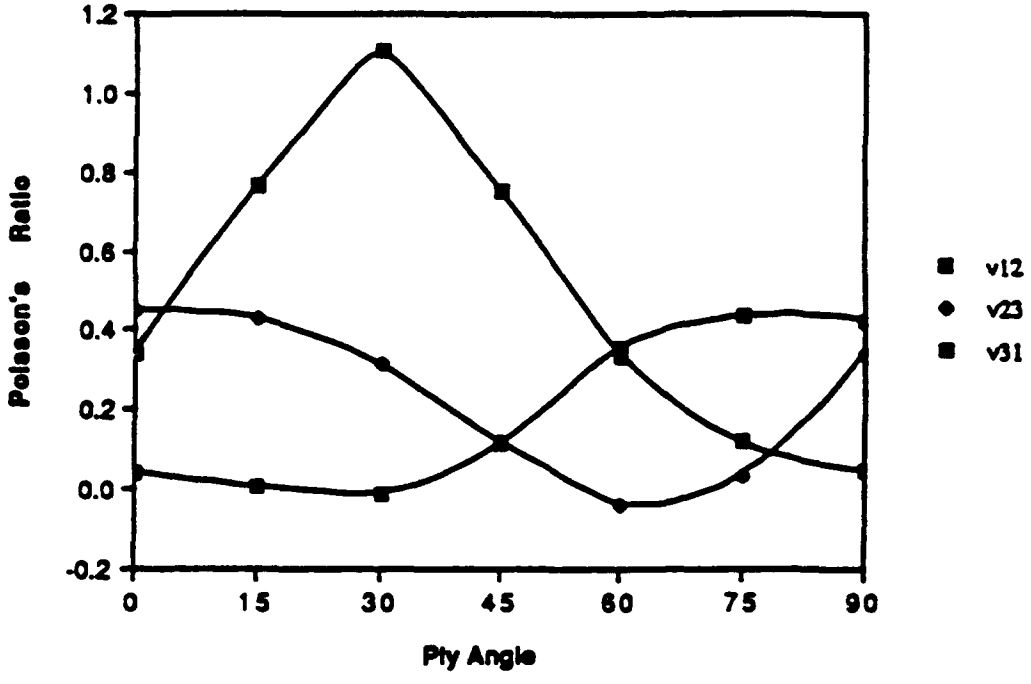

Fig. 29 Poisson's ratios of the Graphite-Epoxy / Kevlar-Epoxy laminates vs Ply-angle. (Analytical)

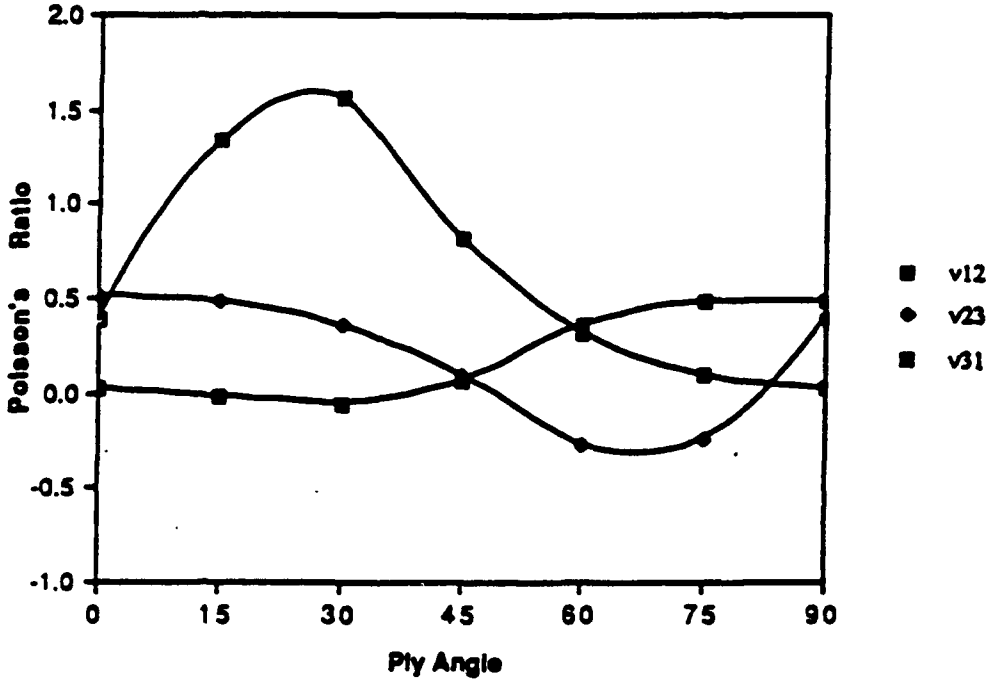

Fig. 30 Poisson's ratios of the Graphite-Epoxy / Glass-Epoxy laminates vs Ply-angle. (Analytical)

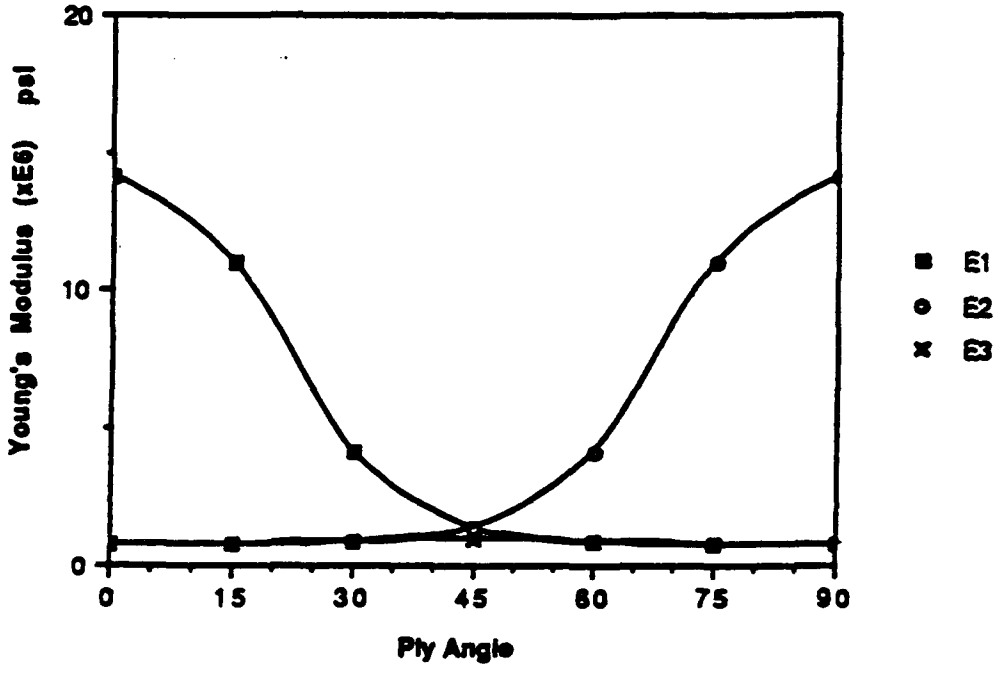

Fig. 31 Young's moduli of the Graphite-Epoxy / Kevlar-Epoxy laminates vs Ply-angle. (Analytical)

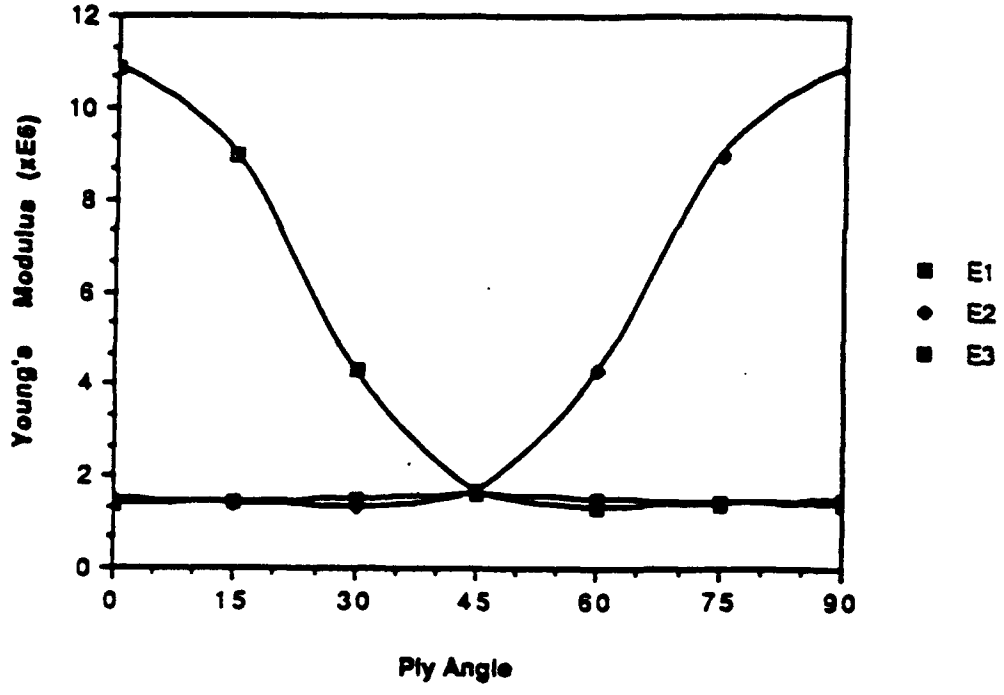

Fiq. 32 Young's moduli of the Graphite-Epoxy / Glass-Epoxy laminates vs Ply-angle. (Analytical)

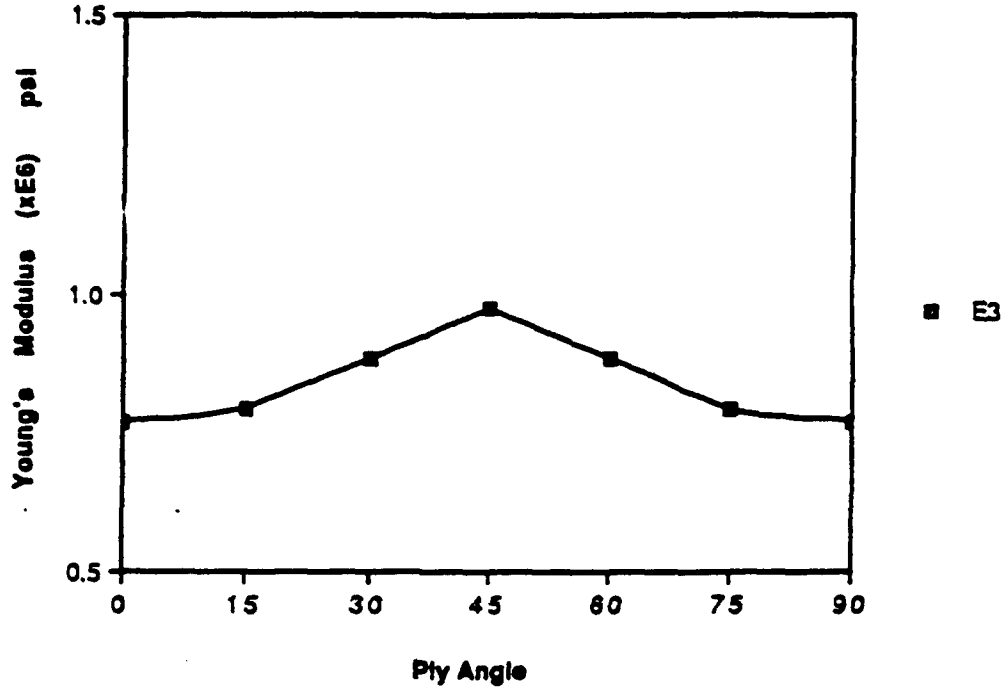

Fig. 33 Young's moduli along the thickness of the Graphite-Epoxy / Kevlar-Epoxy laminates vs Ply-angle. (Analytical)

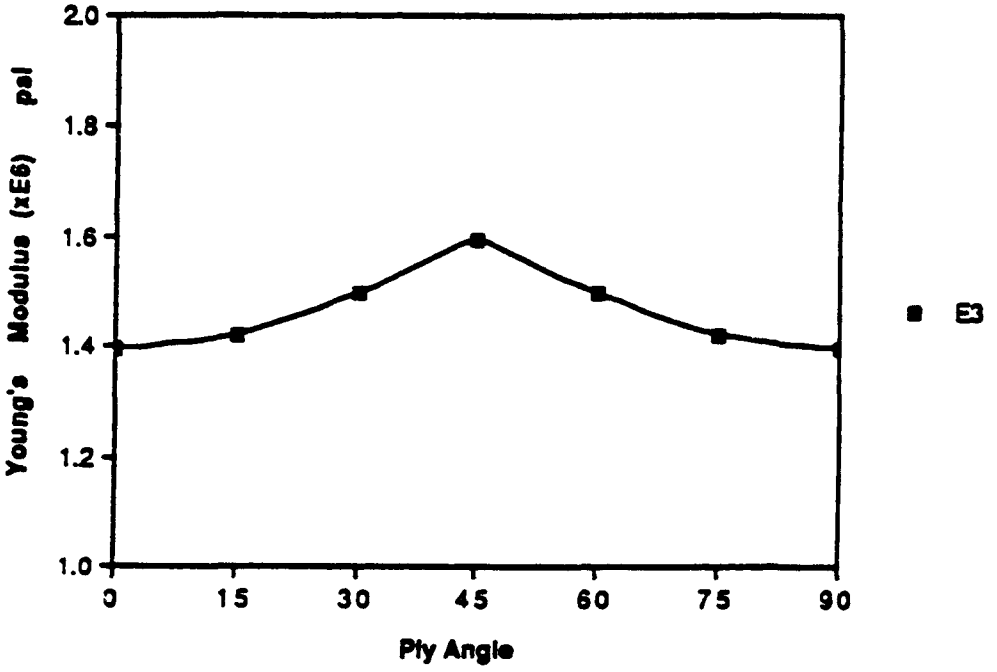

Fig. 34 Young's moduli along the thickness of the Graphite-Epoxy / Glass-Epoxy laminates vs Ply-angle. (Analytical)

Elasticity calculations of E_1 and E_2 were carried out and were very close to the values obtained by ELAS, indication that the model used was satisfactory and needed no refinement.

2. Stress Analysis of Double Ligament Tensile (DLT) Test

From the loading conditions and the shape of a *DLT* specimen, it may be easily seen that tensile stresses act on the ligament region. But the stress distribution in the ligament region should be examined to get the exact stress vs. strain behavior of the specimen. The design of a DLT specimen has been shown in Fig. 5, in which the dimensions of the specimen is 0.4" x 0.4" x 2.0". Two ligaments were formed by cutting in slots from the top and bottom of the specimen blank. Cross sectional view of a DLT specimen has been shown in Figure 6. The specimen was held firmly in the both sides, and the center region was pushed by a square punch with a dimension of 0.4" x 0.4". To record the displacements of ligament regions, strain gauges Micro-Measurements series EA–13–031 CF–120 were used.

The stress analysis in the ligament section was carried out with a Finite Element method and the aid of a VAX/VMS computer. The flow chart of the finite element analysis program used in this study was shown in Fig. 35. Two variables, the ligament length and ligament width, were examined in the geometry of double ligament tensile specimens. Fig. 36 illustrated the meshes and loading condition of the finite element analysis. The stresses at the ligament ends were very high while the variation in the middle of the ligament was small. Fig. 37 and 38 show the large stress concentration at the ligament ends and the effect of changing the ligament thickness and ligament length on the uniformity of the stress.

Results of this analysis together with the experimental results have been included in Fig. 7, 8 and 9.

Even if the stresses in the slot ends can be reduced by making the slots round stress concentration at the slot ends is still too high to be ignored without making the ligament region extremely small. When testing brittle materials like the composite materials used in this study, fracture always occurred at the end of slots due to stress concentrations. This fact indicates that the DLT test is not accurate in determining the strength properties of brittle materials beyond their elastic limits. The other restrictions are the size of strain gauge and difficulty in preparing specimens. Small errors in the shapes and dimensions of the specimens may result in large stress variation in the slot ends. Though the stress concentration in the slot ends is a problem in determining fracture strength of brittle materials, the stresses in the middle of the ligament region are very uniform in the elastic range. Thus the DLT test is deemed useful in determining elastic constants of thin materials, but not the strength properties.

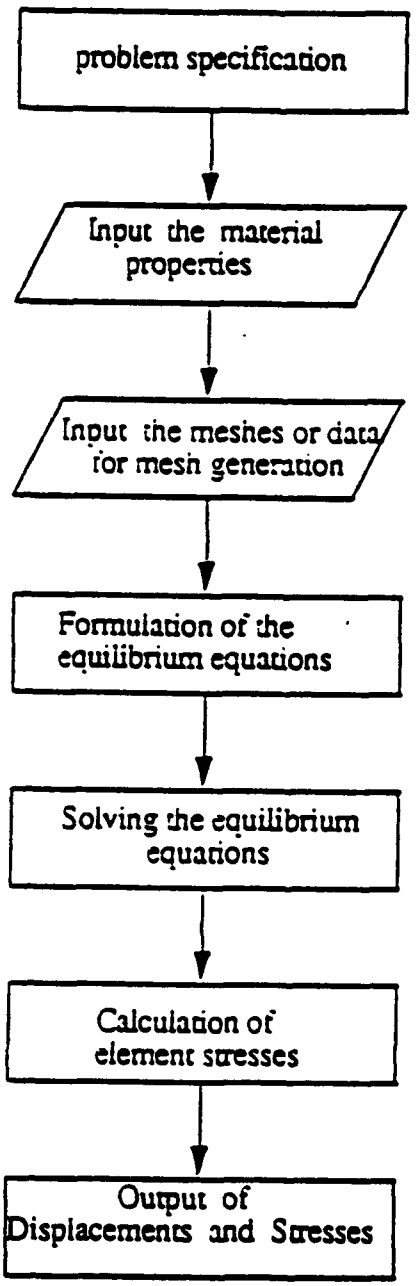

Fig. 35 The flow chart of a finite element program.

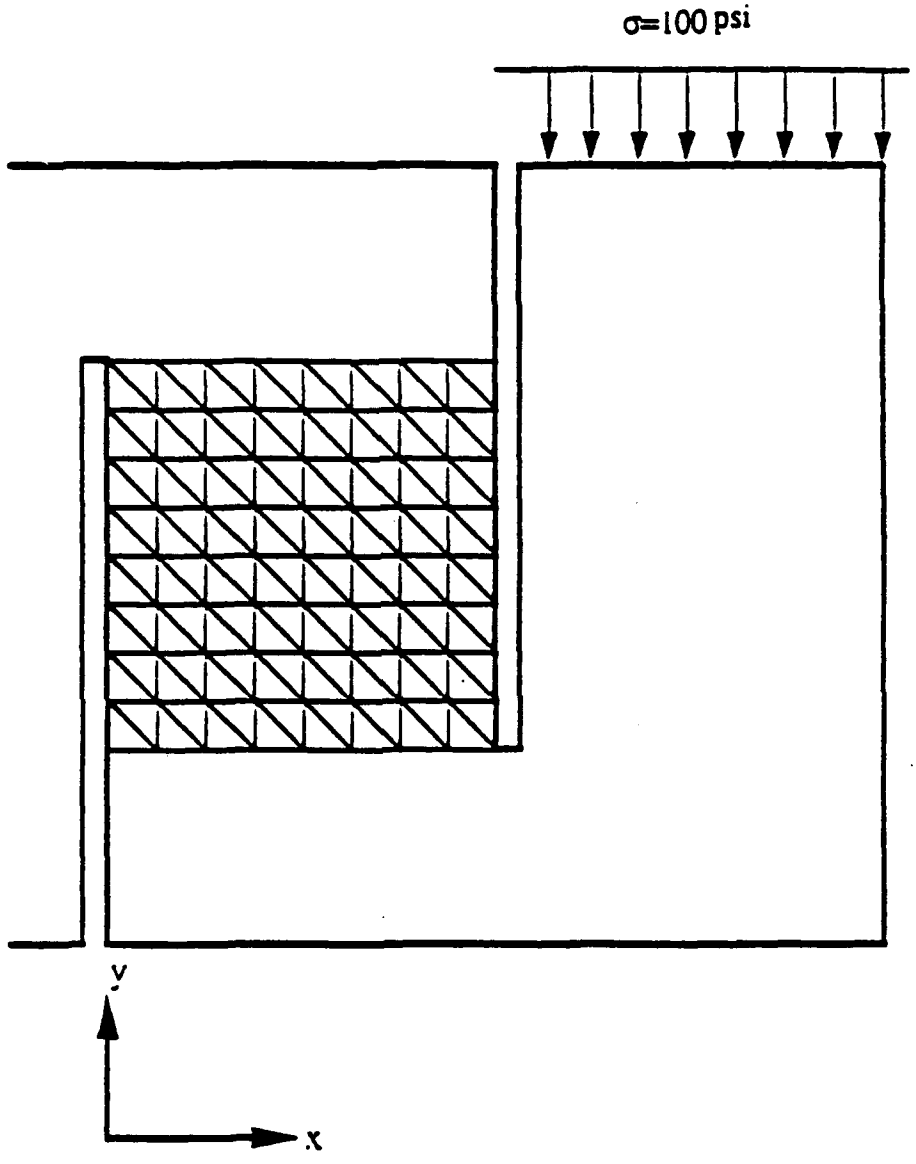

Fig. 36 Finite element meshes in the ligament of a DLT specimen.

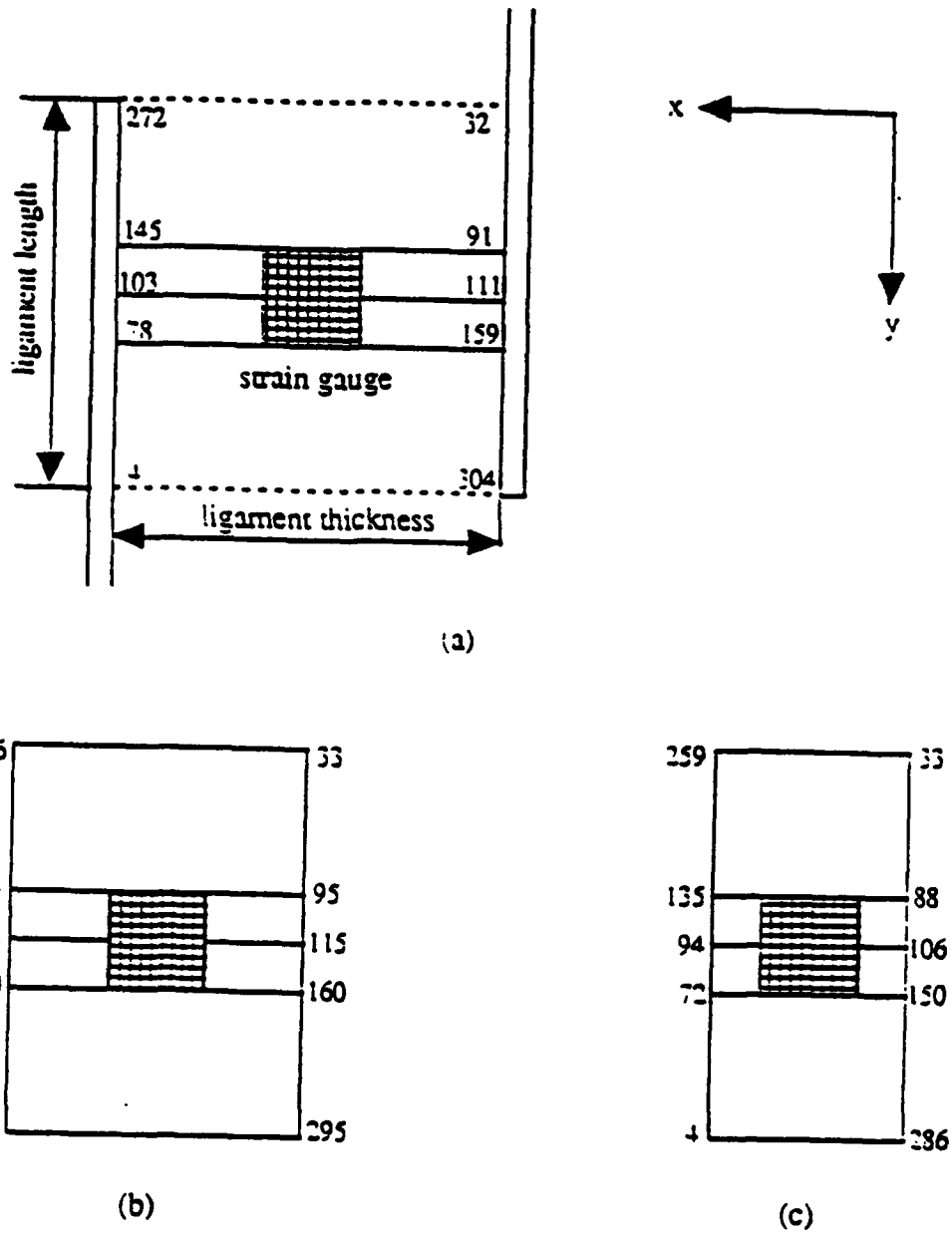

Fig. 37 Stress distributions around the ligament.
a) stress = 100 psi, ligament length = 0.2 in., and ligament thickness = 0.20 in.
b) stress = 100 psi, ligament length = 0.2 in., and ligament thickness = 0.15 in.
c) stress = 100 psi, ligament length = 0.2 in., and ligament thickness = 0.10 in.

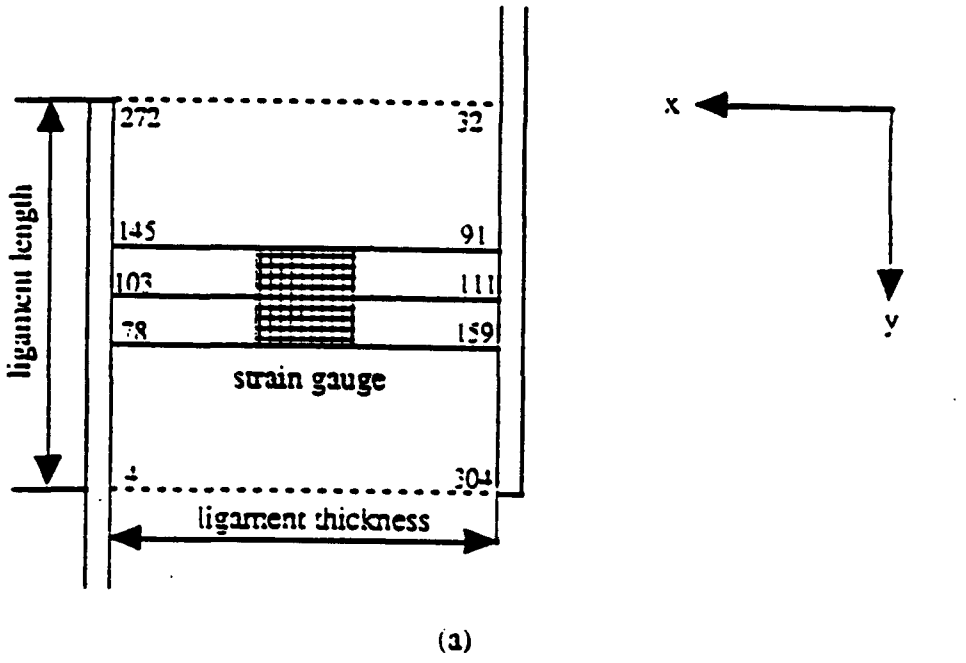

Fig. 38 Stress distributions around the ligament. a) stress = 100 psi, ligament length = 0.20 in., and ligament thickness = 0.20 in. b) stress = 100 psi, ligament length = 0.15 in., and ligament thickness = 0.20 in. c) stress = 100 psi, ligament length = 0.10 in., and ligament thickness = 0.20 in.

CONCLUSIONS

1. Elastic properties along the thickness direction of a hybrid laminated angle-ply composite are significantly different from the transverse properties. In particular, Youngs modulus, is higher than the transverse modulus and the Poisson's ratios involving the thickness direction may become negative for a certain range of ply angle.
2. Experimental values of elastic constants both in thickness tension and thickness compression agree well with analytically determined values indicating the adequacy of the finite element analysis.
3. The double ligament tension test while adequate for obtaining elastic constants was not suitable for determining the tensile strength in the thickness direction because of stress concentration at the ligament ends.
4. As with single fiber-matrix systems, the compressive strength of hybrids along the thickness direction depends greatly on the ply angle with maximum strength for the ± 45° laminates.
5. With the exception of the 0° and ± 45° angles, laminates loaded in compression along the thickness direction exhibit marked "plastic" behavior with the ± 15° laminates showing the greatest plasticity.
6. During the plastic deformation the ply angle undergoes progressive increase towards the 45° by a reverse scissoring mechanism.